JOURNAL OF MATERIALS SCIENCE **38** (2003) 1543–1549

Effect of molybdenum on grain growth of W-Mo-Ni-Fe heavy alloys

CHEN-SHENG HSU
Department of Materials Science and Engineering, National Huwei Institute of Technology, Yulin 632, Taiwan

SHUN-TIAN LIN
Department of Mechanical Engineering, National Taiwan University of Science and Technology, Taipei 106, Taiwan
E-mail: stlin@mail.ntust.edu.tw

The grain growth phenomena of tungsten heavy alloys with various concentrations of Mo were investigated. The early formation of a eutectic liquid phase with the alloying of Mo to W-Ni-Fe facilitated growth and spheroidization of tungsten grains in the initial stage of isothermal hold. However, when the concentration of molybdenum was so high as to leave behind non-dissolved Mo grains, coalescence of W grains around Mo grains resulted in the formation of larger W-Mo grains having Mo-rich cores. These larger grains later grew at the expense of the smaller grains and grain growth was statistically very fast. During grain growth in the later stage of isothermal hold, W had a higher potential than Mo to precipitate from the liquid phase onto the grains. This competitive behavior led to the gradual accumulation of Mo atoms in the liquid phase, which not only retarded the growth of grains, but also caused precipitation of intermetallic phases in the interfaces between the solid grains and liquid phase during cooling.

1. Introduction

For most liquid phase sintered systems, the liquid phase is not in equilibrium with the solid grains when the liquid phase is first formed [1–4]. The microstructure evolves dramatically in the initial stage of liquid phase sintering in a trend toward the equilibrium structure. The characteristics of microstructure such as contiguity of grains and dihedral angle between neighboring grains gradually decrease as the liquid phase progressively penetrates the boundaries between grains [3–5]. Penetration of the liquid phase into the grain boundaries takes place by a combination of capillarity and reaction such that the chemistry of the liquid phase constantly changes with the evolution of microstructure [1, 2].

Alloying of Mo to the W-Ni-Fe alloys can lower the formation temperature and alter the chemistry of the liquid phase, because the eutectic temperatures of binary Mo-Ni, Mo-Fe, W-Ni, and W-Fe alloys are 1320°C, 1460°C, 1455°C, and 1533°C, respectively [6]. A first liquid phase with Ni, Fe and Mo as the major components will form at a lower temperature when Mo is added to W-Ni-Fe alloys. On the other hand, previous studies have indicated that the concentration of W is comparable with that of Mo in the liquid phase when W-Mo-Ni-Fe alloys are sintered for a sufficiently long time [1, 2]. Hence, it can be inferred that the chemistry of the liquid phase gradually transits from the first liquid phase being primarily composed of Ni, Fe, and Mo to the principal liquid phase being composed of Ni, Fe, W, and Mo during the progression of liquid phase sintering. Due to such a fact, growth and spheroidization of grains during the initial stage of liquid phase sintering will be greatly altered by the addition of Mo to W-Ni-Fe alloys. The boundary migration velocity of Mo-Mo grains for Mo-Ni (0.67 μm/min) [7] is more than three times larger than that of W-W grains for W-Ni (0.18 μm/min) [8] at 1500°C. Coalescence of Mo grains is expected to be more frequent than W grains. Nevertheless, refined microstructure are usually obtained when Mo was added to W-Ni-Fe alloys.

One of the observations for tungsten heavy alloys containing high concentrations of Mo is the existence of a bimodal grain size distribution in the initial stage of isothermal hold [9]. The smaller grains are composed of high concentrations of tungsten, while most of the larger ones have Mo-rich cores [1, 2, 10–12]. The reasons for such an observation have not been well explained by past reports. For example, it was proposed that the larger grains with Mo-rich cores were the consequences of nucleation and growth of grains from the first liquid phase, when Mo first re-precipitated from the liquid phase and W gradually dissolved into the liquid phase [12]. On the other hand, it was also suggested that the existence of the large W-Mo grains having Mo-rich cores was caused by the sinter-bonding of W grains around Mo grains [2], leading to coalescence among grains. In fact, there is a finite probability for neighboring grains to coalesce in liquid phase sintered systems, especially in the initial stage of liquid phase sintering [4]. However, this suggestion still lacks direct evidence.

Based on previous analyses, the roles of Mo in the sintering of tungsten heavy alloys are expected to be multi-fold. The addition of Mo can accelerate microstructural evolution due to the early formation of the first liquid phase. It can also result in the coexistence of the larger and the smaller grains, posing a state of instability that will eventually lead to excessive grain growth. Nevertheless, the grain growth rate is reduced due to the transition of the controlling mechanism of grain growth to a newer and slower mechanism. The events of microstructural evolution of W-Mo-Ni-Fe alloys are thus expected to be different from those of W-Ni-Fe alloys. It is due to the complicating roles that Mo plays in W-Ni-Fe alloys that several different and contradictory results can be found in past reports. For example, it was concluded that the addition of Mo to W-Ni-Fe could reduce the interfacial energy between the liquid phase and the solid phase, and, consequently, lower contiguities of grains [13]. Both the tensile strength and ductility were enhanced due to the lowering of contiguity of grains. However, it was generally found that the addition of Mo to W-Ni-Fe resulted in heavy alloys exhibiting higher strengths and lower ductilities whose combinations were similar to those of cold-worked ones [14]. Such different conclusions could arise from the facts that different concentrations of Mo were added to the W-Ni-Fe alloys, and/or that the observations were carried out for test specimens that were exposed to different stages of the sintering event. Hence, to identify the exact roles of Mo in the liquid phase sintering of W-Mo-Ni-Fe alloys, the composition of Mo in W-Mo-Ni-Fe alloys was varied, such that the concentrations of Mo in the liquid phase ranged from under-saturation to super-saturation. The microstructures of these alloys in different stages of liquid phase sintering were analyzed.

2. Experimental procedures

Four different compositions of tungsten heavy alloys were investigated in this study. The compositions were designed to have the equivalent volume fraction of Ni and Fe in the powder state, but have various volume fractions of Mo. The compositions of these four alloys expressed in weight percent were W-6.5Ni-2.8Fe, W-1.9Mo-6.7Ni-2.9Fe, W-8Mo-7Ni-3Fe, and W-22.4Mo-7.8Ni-3.4Fe. Elemental W, Mo, Ni, and Fe powders were used as the starting powders. The characteristics of these four powders are shown in Table I. These powders were mixed and blended in a plastic jar for 16 hours in the existence of heptane and paraffin wax (1.5 wt pct), using 304 stainless steel balls. The powder slurry was then dried at 80°C and the granules were sieved with a screen of 70 mesh. Cylindrical specimens having the dimensions of 15 mm in diameter and 3 mm in height were die-pressed with a pressure of 110 MPa. The specimens were then sintered in a tube furnace using a thermal profile that combined the functions of dewaxing, oxide reduction, decarburization, and densification. The thermal profile was heating at 3 K/min to 350°C, held for 60 minutes, and then 3 K/min to 500°C, held for 60 minutes. This schedule was followed directly by heating at 10 K/min to 1000°C, held for 60 minutes, and then heating at 10 K/min to 1500°C, held for either 5, 15, 30, 60, 120, 180, or 240 minutes. One group of specimens was sintered with the same profile, except that the sintering temperature was 1380°C and the isothermal hold was 0 minute. All the specimens were furnace-cooled. Hydrogen atmosphere was maintained until the last 10 minutes (or 5 minutes for an isothermal holding time of 5 minutes) of the isothermal hold, when the atmosphere was changed to argon.

TABLE I Characteristics of the elemental powders used in this study

Property	W	Mo	Ni	Fe
Vendor	Korea tungsten	Climax	INCO	BASF
Designation	KM-8	OMP-6	123	OM
Purity Wt pct	99.95	99.8	99.8	97.8
Mean particle size, μm	4	5	11	4
Tap density g/cm^3	2.8	2.2	4.7	4.3
Major impurities	O	Si, Fe, Sn	C, O, Fe	N, C, O

To identify the formation temperature of the liquid phase for each composition, differential thermal analysis (DTA) was carried out for all four alloys. Green compacts prepared by mixing the elemental powders were used as the tested specimens, which had weights of about 30 mg. The heating rate and cooling rate during test were maintained at 10 K/min. An argon gas of high purity (99.999%) was used as the protective atmosphere.

The sintered specimens were ground and polished to a depth of approximately 0.5 mm from the surface, and etched with Murakami's solution (10 g $K_3Fe(CN)_6$, 10 g KOH, and 100 g H_2O) for approximately 1 minute. Back-scattered electron images (BEI) of the etched specimens were examined along with electron probe microanalysis (EPMA), using a scanning electron microscope (SEM, JEOL JXA-8900R) operated at an accelerating voltage of 20 kV. The recorded intensities of Ni K_α, Fe K_α, Mo L_α, and W L_α radiations were taken for calculating the concentrations of Ni, Fe, Mo, and W, respectively, in selected areas. The reported values were the averages of three tested areas. The uncertainty in this composition analysis was about ±1 atomic pct and the effective excitation volume was about 1 μm in diameter. The determination of phase composition was carried out for domains larger than 2 μm in size to avoid interference from the adjacent domains. Grain size distribution of W-Mo grains was determined by measuring the longest dimension of at least 200 grains, in which the dimension of each grain was determined by multiplying the measured value by 1.5.

3. Results

3.1. Thermal analysis

Fig. 1 shows the DTA patterns of the four alloys, which include the patterns of the heating and cooling cycles. It is noted that the absolute quantity of heat flow in the heating process is much larger than that in the cooling process. This difference arises from the fact that

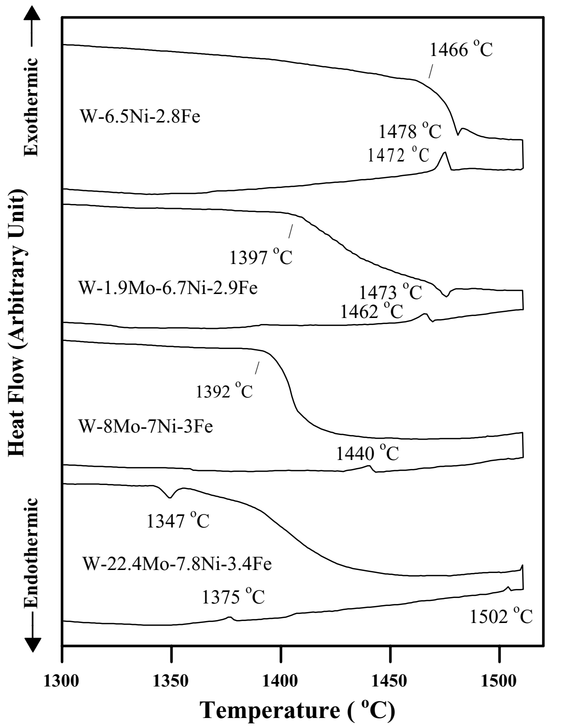

Figure 1 DTA patterns of four alloys investigated in this study.

different sequential steps were involved in heating and cooling tests. The endothermic pattern during heating is associated with alloying of elements as well as melting of the alloy, while the exothermic pattern during cooling is primarily associated with the solidification of the liquid phase. There is a minor endothermic peak occurring at 1347°C for W-22.4Mo-7.8Ni-3.4Fe, which is not obvious for the other two alloys having lower concentrations of Mo. It is noted that the eutectic temperature of Ni-Mo is 1320°C [6] and the magnitude of this endothermic peak is relatively smaller than the principal endothermic peak that takes place at higher temperatures. Thus, it can be inferred that this smaller endothermic peak is associated with the formation of the first liquid phase that is primarily composed of Ni, Fe, and Mo. In fact, the ternary phase diagram of Mo-Ni-W shows that a liquid phase, which is primarily composed of Ni and Mo (35 mol%), forms at 1327°C [15].

With further increase in test temperature, the slopes of these curves drastically change, and the endothermic patterns are larger in scale, which were due to the formation of the principal liquid phases. Such a transition of slope occurs at a lower temperature for the alloy having a higher concentration of Mo. The transitions of slopes finally end up with sharp endothermic peaks, which occur at 1478°C and 1473°C, respectively, for W-6.5Ni-2.8Fe and W-1.9Mo-6.7Ni-2.9Fe. It can be concluded from the above observations that the principal liquid phases for these four alloys form at a wide range of temperatures and their compositions vary gradually during the ramp to 1500°C. It is also noted that there were two exothermic peaks for W-22.4Mo-7.8Ni-3.4Fe during cooling test, which respectively corresponded to solidification of the liquid phase (1502°C) and precipitation of an intermetallic compound (1375°C), which will be shown in a later section.

3.2. Evolution of microstructure

Fig. 2 shows the microstructures of the specimens sintered at 1380°C, without isothermal hold. There are three relatively different degrees of blackness in these black and white BEI pictures, which respectively designate the W-rich phase, the Mo-rich phase, and the Ni (and Fe)-rich liquid phase in increasing order of blackness. It can be seen from this figure that close to fully dense microstructures had been achieved, irrespective of the fact that the formation temperature of the principal liquid phase was higher than 1380°C for the three alloys having no or low concentrations of Mo (Fig. 1). The grains of the four alloys were relatively similar in dimension and were in a similar scale to the initial grains of W powder. Mo grains could hardly be found in the microstructure for W-8Mo-7Ni-3Fe, while a large fraction of the solid grains were associated with non-dissolved Mo grains for W-22.4Mo-7.8Ni-3.4Fe.

Fig. 3 shows the microstructures of the alloys sintered at 1500°C for 5 minutes. The evolution of microstructure from Fig. 2 to Fig. 3 dictates the major events occurring in the initial stage of isothermal hold when the liquid phase was not in equilibrium with the solid grains. As the microstructures of these four alloys shown in Fig. 3 are greatly different, it can be inferred that there should be dramatically different phase partitioning mechanisms subsequent to the formation of the principal liquid phases. The grains of W-6.5Ni-2.8Fe were angular in shape and bonded together to a large fraction, while spheroidal grains dominated the microstructure of W-1.9Mo-6.7Ni-2.9Fe, though their compositions only differed slightly. The microstructure of W-1.9Mo-6.7Ni-2.9Fe resembled those of traditional W-Ni-Fe heavy alloys sintered for a substantially long time, only with smaller grains. This observation implied that penetration of liquid phase into the grain boundaries, causing subsequent growth and spehroidization of grains, had effectively taken place for W-1.9Mo-6.7Ni-2.9Fe but not for W-6.5Ni-2.8Fe. Such different observations arose from the fact that the addition of a low concentration of Mo to the alloy altered the composition of the first liquid phase and reduced the formation temperature of the liquid phase. On the other hand, the microstructures of W-8Mo-7Ni-3Fe and W-22.4Mo-7.8Ni-3.4Fe were similar, but were distinctively different from those two discussed previously. Not only were the grains irregular in shape, but also the grains had a bimodal-like distribution. These two groups of grains inherently had different forms of existence, wherein most of the larger grains had Mo-rich cores (61 mol% Mo near the core and 27 mol% Mo near the rim) while the smaller ones were associated with very high concentrations of tungsten (less than 1 mol% Mo).

Fig. 4 shows the microstructures of the four alloys sintered at 1500°C for 240 minutes. The bimodal distributions of grain size for W-8Mo-7Ni-3Fe and W-22.4Mo-7.8Ni-3.4Fe had vanished and the grains became spheroidal in shape for such an extended

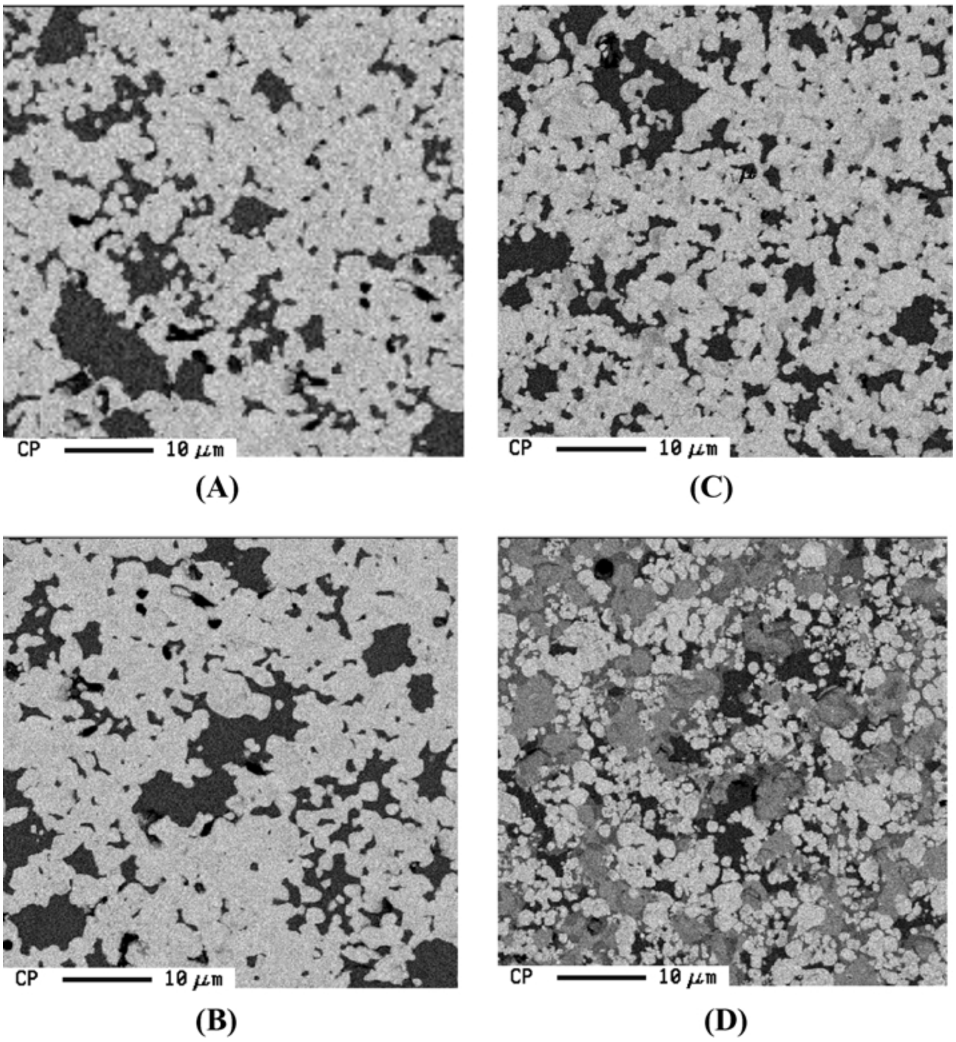

Figure 2 Microstructures of alloys sintered at 1380°C, without isothermal hold. (A) W-6.5Ni-2.8Fe, (B) W-1.9Mo-6.7Ni-2.9Fe, (C) W-8Mo-7Ni-3Fe, and (D) W-22.4Mo-7.8Ni-3.4Fe.

isothermal hold, only with their mean grain sizes being lower than those of W-6.5Ni-2.8Fe and W-1.9Mo-6.7Ni-2.9Fe. The microstructure of W-6.5Ni-2.8Fe can hardly be differentiated from that of W-1.9Mo-6.7Ni-2.9Fe though its microstructural evolution was slightly delayed in the initial stage of isothermal hold. By comparing this observation with that shown in Fig. 2, it can thus be inferred that the microstructural evolutions of W-6.5Ni-2.8Fe and W-1.9Mo-6.7Ni-2.9Fe differed primarily in the temperatures at which their first liquid phases were formed (Fig. 1), and, accordingly, the chemistries of their first liquid phases. Such differences gradually became insignificant with the extension of isothermal hold when tungsten gradually dissolved into the liquid phase and became the major element dissolved in the liquid phase. In fact, the concentrations of W in the liquid phase for an isothermal hold of 240 minutes were 8.7 mol% and 8.4 mol% for W-6.5Ni-2.8Fe and W-1.9Mo-6.7Ni-2.9Fe, respectively.

There was one minor exothermic peak occurring at 1375°C in the cooling test of DTA for W-22.4Mo-7.8Ni-3.4Fe (Fig. 1), which was previously mentioned to be associated with the formation of an intermetallic compound during cooling. Fig. 5 shows the existence of Mo-rich layers around the W-Mo grains for W-22.4Mo-7.8Ni-3.4Fe sintered at 1500°C for 240 minutes. The composition of this phase was found to be composed of 18.8 mol% W, 30.2 mol% Mo, 34.1 mol% Ni, and 16.9 mol% Fe, which is approximately equivalent to $(W_{0.4}Mo_{0.6})(Ni_{0.7}Fe_{0.3})$. It was also observed that the relative thickness of this Mo-rich layer increased with increase in isothermal hold [16], which could be the primary cause for the deterioration of tensile properties for an extended isothermal hold [5]. This observation indicates that this intermetallic layer was not merely the consequence of slow cooling rate, but also that of the prior accumulation of Mo atoms in the liquid phase with increase in isothermal hold. In fact, when the isothermal hold increased from 5 to 240 minutes, the concentration of Mo in the binder phase increased from 1.9 mol% to 5.1 mol% for W-8Mo-7Ni-3Fe, and from 1.2 mol% to 6.3 mol% for W-22.4Mo-7.8Ni-3.4Fe.

3.3. Statistical analysis of grain growth

Fig. 6 shows the variation of mean grain size with increase in isothermal hold for these four alloys. The data shown in this figure were not fitted linearly in the log-log plot as the data points of W-8Mo-7Ni-3Fe and W-22.4Mo-7.8Ni-3.4Fe deviate substantially from linearity. For W-6.5Ni-2.8Fe, its mean grain size gradually surpassed that of W-1.9Mo-6.7Ni-2.9Fe with

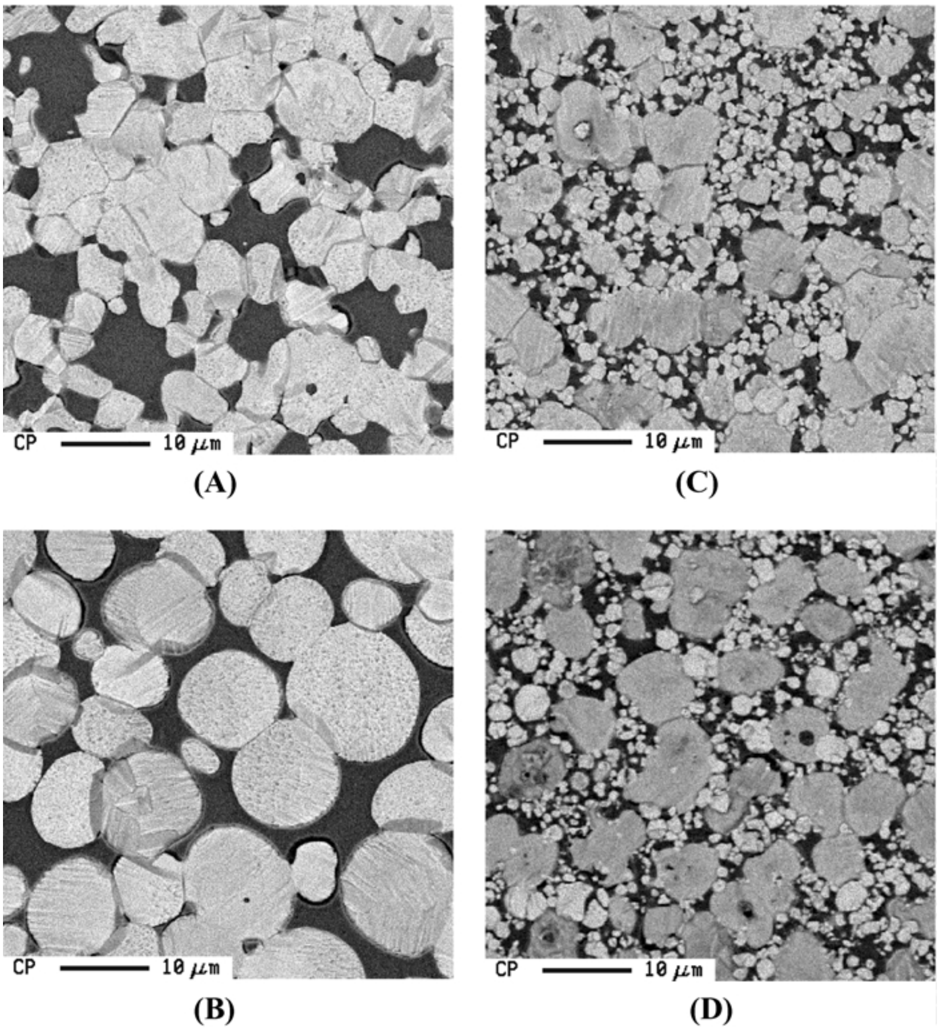

Figure 3 Microstructures of alloys sintered at 1500°C for 5 minutes. (A) W-6.5Ni-2.8Fe, (B) W-1.9Mo-6.7Ni-2.9Fe, (C) W-8Mo-7Ni-3Fe, and (D) W-22.4Mo-7.8Ni-3.4Fe.

increase in isothermal hold, though the microstructural evolution of W-6.5Ni-2.8Fe was delayed in the initial stage of isothermal hold. There are three distinct stages of grain growth for the two alloys containing higher concentrations of Mo (W-8Mo-7Ni-3Fe and W-22.4Mo-7.8Ni-3.4Fe). Initially, their mean grain sizes were statistically much smaller than those of W-1.9Mo-6.7Ni-2.9Fe and W-6.5Ni-2.8Fe, due to the abundant existence of smaller grains in their microstructures. The coexistence of the larger and smaller grains was in a state of great instability, which caused the fast disappearance of the smaller grains in a short interim during the isothermal hold. Accordingly, their mean grain sizes abruptly boosted up for an isothermal hold slightly longer than 30 minutes. Subsequent to the disappearance of the smaller grains, which took place for an isothermal hold of about 120 minutes, the rate of grain growth decreased and the mean grain sizes leveled off. The observation of similar grain growth patterns for W-8Mo-7Ni-3Fe and W-22.4Mo-7.8Ni-3.4Fe is very striking as they differ very significantly in composition. It is thus clear that there is a transitional concentration of Mo for the evolution of microstructure, above which the excess Mo atoms do not effectively affect the grain growth behavior of W-Mo-Ni-Fe alloys. These excess Mo atoms are believed to exist as solid grains during liquid phase sintering.

4. Discussion

Based on previous analyses, the effects of Mo on the microstructural evolution of tungsten heavy alloys have been identified, whose relative degrees of significance depend not only on the concentration of Mo in the alloy, but also on the extent of isothermal hold. These effects are summarized and discussed as follows.

4.1. Growth and spheroidization of grains

In the progress of microstructural evolution, the grains of tungsten and molybdenum were initially randomly bonded together by the activation of Ni and Fe. When a liquid phase formed, it could penetrate the grain boundaries between W and W, between W and Mo, and between Mo and Mo, inducing spheroidization and growth of grains. The liquid phase penetrates into grain boundaries by a combination of reaction and capillarity such that a liquid phase highly saturated with an element generally will not readily corrode and penetrate the boundaries formed by grains of this element [4]. The liquid phase of W-6.5Ni-2.8Fe formed at higher temperatures (1466°C to 1478°C) than the other three alloys. It contained a high concentration of W, which was unfavorable for the penetration of liquid phase into the grain boundaries of W. In addition, the time allowed for the penetration of liquid phase into the grain

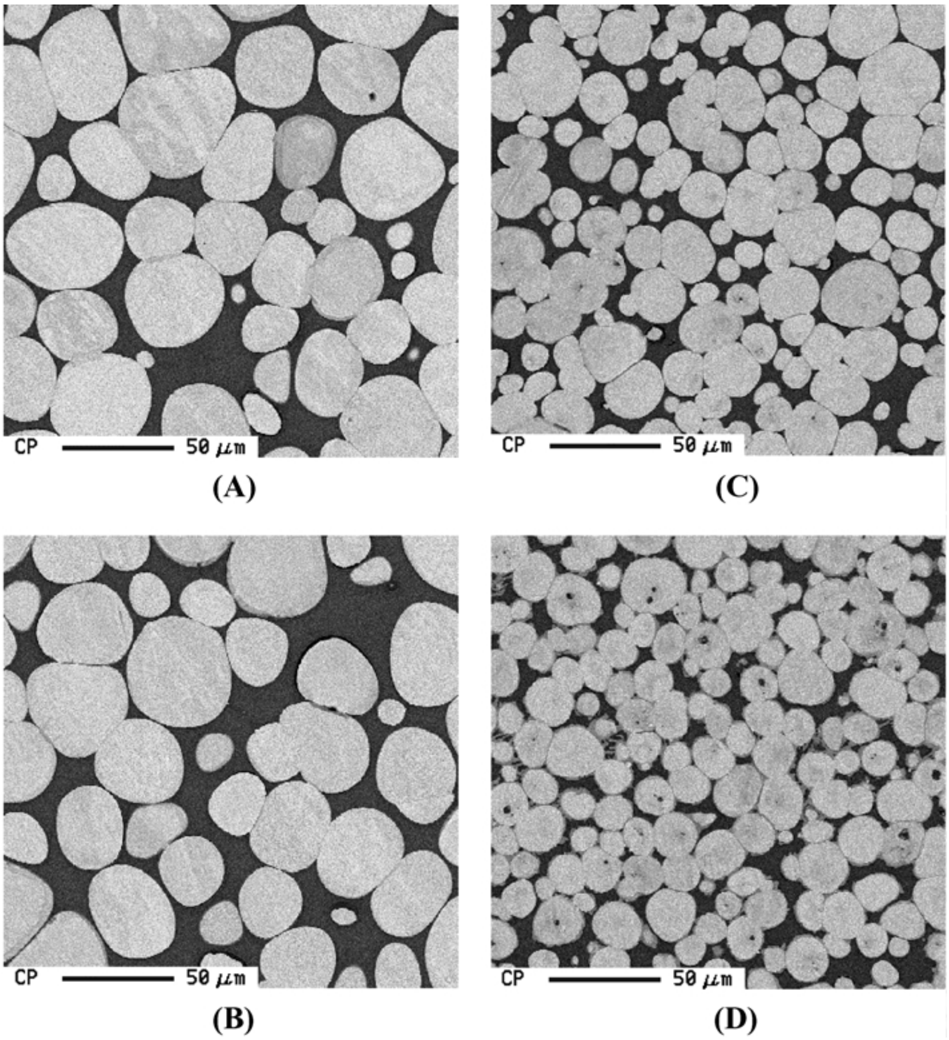

Figure 4 Microstructures of alloys sintered at 1500°C for 240 minutes. (A) W-6.5Ni-2.8Fe, (B) W-1.9Mo-6.7Ni-2.9Fe, (C) W-8Mo-7Ni-3Fe, and (D) W-22.4Mo-7.8Ni-3.4Fe.

boundaries was also shorter. Accordingly, the W grains were severely bonded together when the isothermal hold was short (Fig. 3A). In fact, 1600°C was found to be a transitional temperature for the penetration of Ni into polycrystalline W when the test was carried out for a short test time [17]. Below 1600°C, penetration or non-penetration of the liquid phase into the boundaries of W grains could mutually take place, which depended on the relative mis-orientation angle of the neighboring grains.

On the other hand, the addition of Mo to the heavy alloys facilitated the formation of a Mo-rich liquid phase at a lower temperature, which was favorable for the penetration of the liquid phase into the boundaries between W grains. The liquid phase, which was originally low in the concentration of W, gradually penetrated the boundaries between W and W grains. Along with the penetration of liquid phase into the boundaries between W grains, the liquid phase gradually transited from one that was rich in Mo to one rich in both Mo and W. Hence, spheroidization and growth of tungsten grains actively proceeded in the initial stage of isothermal hold. Such an effect could be activated even when the alloying concentration of Mo was as low as 1.9 wt% in the alloy (Fig. 3B). It is noted that elemental powders were used in this study that a fraction of Mo powder added to this alloy might have not participated in the formation of liquid phase. In fact, when a pre-alloyed Ni-Fe-Mo powder was used as the liquid phase precursor, an alloying concentration as low as 0.84 wt% Mo was found effective in promoting the spheroidization and reducing the contiguity of grains [13].

4.2. Coalescence of grains

There existed lots of Mo grains surrounded by W grains for W-22.4Mo-7.8Ni-3.4Fe sintered at 1380°C (Fig. 2). For a W grain and a Mo grain separated by a thin liquid film that is primarily composed of Ni, Fe, and Mo, there exists a chemical potential difference across the thin liquid film that would drive the migration of the grain boundary. If the liquid phase is saturated with Mo, the chemical potential of Mo in the Mo grain is equivalent to that in the liquid phase. There is no tendency leading to a net mass transfer of Mo between the Mo grain and the liquid phase. However, Ni and Fe have the tendency to dissolve into the Mo grain, as the maximum concentrations of Ni and Fe dissolving in Mo are about 2 mol% and 18 mol%, respectively, at 1500°C [6]. On the other hand, the chemical potential of W in the W grain is higher than that in the liquid film since the first liquid phase is low in the concentration of W atoms.

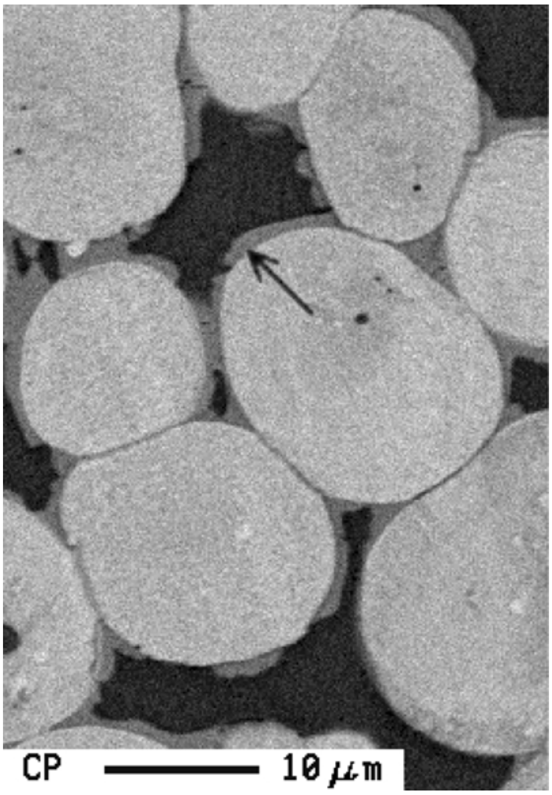

Figure 5 Existence of an interfacial phase between the liquid phase and the grains for W-22.4Mo-7.8Ni-3.4Fe sintered at 1500°C for 240 minutes.

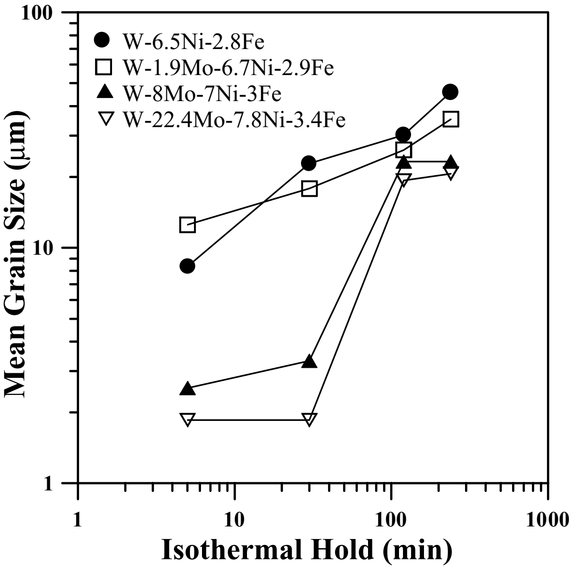

Figure 6 Variation of mean grain size with isothermal hold in log-log scale for the four alloys investigated in this study.

The W atoms in the W grain accordingly have a strong tendency to dissolve into the liquid phase. The transport of Ni, Fe, and W toward the direction of the Mo grain results in the migration of the grain boundary (and thin liquid film) toward the W grain. Such grain boundary migration induced by chemical potential gradients results in coalescence of these two W and Mo grains.

The grain boundary migration will continue until the liquid phase are completely dissolved into the newly precipitated region of the large coalesced grain, should their local quantities be low. If the quantity of the liquid phase is higher, the coalescence of grains in the three-dimensional space will eventually lead to the entrapment of the excessive liquid phase within grain junctions. The pockets of liquid phase within larger grains can be observed in Fig. 3C and D.

5. Conclusion

The roles of Mo in the sintering of W-Mo-Ni-Fe heavy alloys are multi-fold, whose effects depend on the concentration of Mo added to the alloy and the stage of isothermal hold. It accelerates the early formation of a liquid phase that is primarily composed of Ni, Fe, and Mo during the ramp to the sintering temperature, which promotes growth and spheroidization of grains in the initial stage of isothermal hold. Nevertheless, when its concentration is high enough to leave alone non-dissolved Mo grains, fast migration of boundaries between Mo and W grains facilitates coalescence of W grains around Mo grains, which results in larger grains with Mo-rich cores. Moreover, the liquid phase has a greater tendency to penetrate the boundaries between W grains. Accordingly, the liquid phase gradually changes its composition from one that is primarily composed of Ni, Fe, and Mo to one that is composed of Ni, Fe, Mo, and W. Such concurrent progression of microstructure leads to the bimodal distribution of grain size. The coexistence of larger and smaller grains poses a state of instability, which eventually induces the fast grain growth in the intermediate stage of isothermal hold.

References

1. T. Y. CHAN and S. T. LIN, *Metall. Mater. Trans.* A, **29A** (1998) 2885.
2. C. S. HSU, P. C. TSAI and S. T. LIN, *ibid.* **32A** (2001) 95.
3. H. RIEGGER, J. A. PASK and H. E. EXNER, in "Sintering Processes," vol. 13, edited by G. C. Kuczynski (Plenum Press, New York, 1980) p. 219.
4. R. M. GERMAN, in "Sintering Theory and Practices" (John Wiley & Sons, New York, 1996) p. 248.
5. T. Y. CHAN and S. T. LIN, *J. Mater. Sci.* **35** (2000) 3759.
6. C. J. SMITHELL and E. A. BRANDES, "Metal Reference Book," 5th ed. (Butterworth and Co., London, 1977) p. 606, 707, and 740.
7. W. H. RHEE, Y. J. BAIK and D. Y. YOON, *Acta Metall. Mater.* **41** (1993) 1263.
8. D. N. YOON and W. J. HUPPMANN, *Acta Metall.* **27** (1979) 973.
9. A. BOSE and R. M. GERMAN, *Metall. Trans.* A **19A** (1988) 3100.
10. P. B. KEMP and R. M. GERMAN, *Metall. Mater. Trans.* A **26A** (1995) 2187.
11. *Idem.*, *J. Less-com. Met.* **175** (1991) 353.
12. H. D. PARK, W. H. BAIK, S. J. JOONG and D. Y. YOON, *Metall. Mater. Trans.* A **27A** (1996) 3120.
13. J. H. HUANG, G. A. ZHOU, C. Q. ZHU, S. Q. ZHANG and H. Y. LAI, *Mater. Let.* **23** (1995) 47.
14. A. BOSE and R. M. GERMAN, *Metall. Trans.* A **21A** (1990) 1325.
15. P. VILLARS, A. PRINCE and H. OKAMOTO, "Handbook of Ternary Alloy Phase Diagrams," Vol. 10 (ASM International, Materials Park, OH, 1994) p. 12555.
16. K. H. LIN, C. S. HSU and S. T. LIN, *J. Refrac. Metals Hard Mater.* **20** (2002) 401.
17. V. GLEBOVSKY, B. STRAUMAL, V. SEMENOV, V. SURSAEVA and W. GUST, *High Temp. Mater. Proc.* **14** (1995) 67.

Received 5 December 2001
and accepted 25 November 2002